Calculations and measurements of the spectral radiance of the solar aureole

By REINER EIDEN, *Meteorologisch-Geophysikalisches Institut, Johannes Gutenberg-Universität, Mainz*

(Manuscript received September 1, 1967; revised Dec. 11, 1967)

ABSTRACT

The application of the theory of primary scattering to describe and interpret the spectral distribution of the sky radiance is discussed. It is shown that within the solar aureole the influence of the scattering of higher order can be neglected. Theoretical calculations of the spectral distribution of the sky radiance, carried out by Bullrich *et al.* (1965) based on an exponential aerosol size distribution with an upper limiting particle radius $r = 10\ \mu$, have been extended to $r = 150\ \mu$. The detailed study of the influence of these "giant" particles revealed that aerosol particles of $r > 30\ \mu$ have no effect on the sky radiation any more. Representative measurements taken at Mainz, Germany, at the research station Jungfraujoch in the High Alps, Switzerland, and on the island of Maui, Hawaii, are analyzed and interpreted by comparison with theoretical values. Some measurements required a modification of the basic model of the turbid atmosphere. The exponent of the aerosol size distribution generally a constant has to be considered a function of the particle size. Furthermore, the exponent of the aerosol size distribution was found to be a function of height at least in case of subsidence. The exponent increases with height.

Introduction

The radiance of the solar aureole undergoes marked and characteristic variations with the turbidity of the atmosphere. Extreme cases can be observed after volcanic eruptions (Bishop's ring) and large scale forest fires (blue sun). During natural disasters of this type great amounts of dust are lifted into the troposphere and lower stratosphere.

It was the purpose of this study to obtain information on the concentration and size distribution of the large scattering suspensoids in the atmosphere by investigating and measuring the spectral distribution of the absolute radiance of the solar aureole. The latter is also of interest, though only indirectly, to the solar physics. The exact knowledge of the radiance of the solar aureole enables one to correct the measurements of the solar constant or solar corona disturbed by this so-called circumsolar radiation.

Various authors (Günther, 1949; Volz, 1954; Sekihara & Murai, 1961; Newkirk & Eddy, 1964) have already taken measurements of the solar aureole in order to get an information on the aerosol concentration of the atmosphere. A detailed physical explanation of the measurements, however, can be given by the newly made theoretical investigations of the atmospheric scattering processes of sunlight and the calculation of the radiance of skylight (Bullrich *et al.*, 1965).

This study is mainly restricted to the investigation of a normal turbid atmosphere and does not include e.g. phenomena like the brightness of the solar aureole, due to thin ice and water clouds.

Theoretical considerations and calculations

General remarks

Theoretical investigations and calculations of the radiance of the diffuse sky radiation of a turbid atmosphere by Bullrich *et al.* were already avaialable for this study. These calculations have been carried on and fitted for the special requirements of this investigation; they are based upon the theory of primary scattering (Bullrich *et al.*, 1952). The Mie (1908) and the Rayleigh theory resp. have been used for calculating the scattering of sunlight by the individual gas molecules and aerosol particles. The further calculations are based upon a model of the atmosphere which represents average conditions and neglects special physical, chemical, and geometric properties.

The atmosphere is assumed to be an infinite parallel layer. A constant horizontal distribution of the aerosol particles and gaseous molecules is postulated. The vertical distribution of both the gas molecules and the aerosol particles is characterized by a decrease of the number density with height following a exponential law.

The mean aerosol size distribution near the surface can be described according to Junge (1952) by a power law as follows:

$$dN_D(h,r) = n^*(h,r_0)\left(\frac{r}{r_0}\right)^{-\nu^*} d\log r. \qquad (1)$$

$N_D(h, r)$ is called the integral aerosol size distribution or the number density function, i.e. the number of particles with radii from 0 through r per cm^3 in the height h ($h = 0$ at the surface). $n^*(h, r) = dN_D(h, r)/d\log r$ is the differential aerosol size distribution in the height h. r_0 is an arbitrary, but fixed standard radius.

This equation is valid within a radius interval $0.06\ \mu - 0.1\ \mu \leq r \leq 150\ \mu$.

Apart from general considerations (Junge, 1963) the variation of the exponent ν^* of the aerosol size distribution with height is unknown. Since exact data are lacking, the calculation of sky radiation has been based upon the assumption that ν^* is independent of height, i.e. $\nu^*(h) = \text{const}$. This has to be taken into account when measured and computed values are compared. From such a comparison, there results a mean exponent ν^* which averages the aerosol particle size distribution of the entire atmosphere. If, however, the exponent ν^* of the real atmosphere depends on the height, the mean exponent, which averages the entire atmosphere, will differ from the value of ν^* which has been measured right at the observation site.

Fig. 1 shows idealized aerosol size distributions for various exponents ν^* for theoretical treatment. The turbidity of the atmosphere which results from the aerosol size distribution under consideration, is characterized by the spectral turbidity factor according to Linke

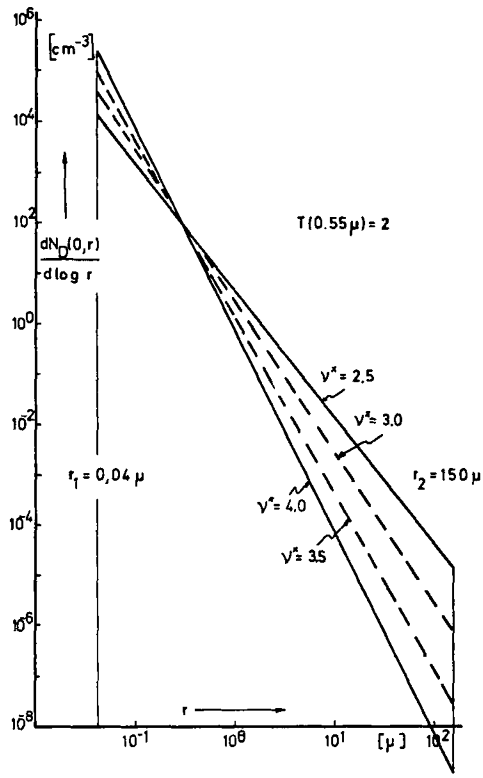

Fig. 1. Model size distribution of atmospheric aerosol particles of a volume of atmospheric air at sea level for different exponents $\nu^* = \text{const}$. Turbidity T (0.55 μ) = 2; r_1 and r_2 lower and upper limiting particle radius.

$$T(\lambda) = (\tau_R(\lambda) + \tau_D(\lambda))/\tau_R(\lambda) \qquad \text{for} \qquad \lambda = 0.55\ \mu.$$

$\tau_R(\lambda)$ and $\tau_D(\lambda)$ are the optical thicknesses of the Rayleigh and the aerosol atmosphere resp., λ is the wavelength. This turbidity factor is indicated in Fig. 1.

Bullrich *et al.* (1965) calculated the sky radiation up to an upper limiting radius of the aerosol size distribution of $r = 10\ \mu$. However, Jaenicke (1966) found from his investigations of the atmospheric layers near the ground that the upper limiting radius is considerably larger and that it must be assumed to be $r = 150\ \mu$ or even more.

Theoretical considerations (van de Hulst, 1957) imply a strong increase of forward scattering with increasing particle radius r. Now, especially in the surroundings of the sun, the forward scattering plays a leading role in the sky radiation. Therefore, theoretical investigations have to take into account the particle size range $10\ \mu \leqslant r \leqslant 150\ \mu$. This requires a continuation of the calculations of Bullrich within the scope of this investigation up to an upper limiting radius of $r = 150\ \mu$. These calculations have to be based on the numerical values of the scattering function $i\ (\varphi, r, \lambda)$ of an individual particle up to this limiting radius. The computation of these scattering functions following the exact Mie equations would have been too time consuming because of the largeness of the particles, even for electronic computers. But using the laws of geometrical optics which can be applied to particles of a radius $r \geqslant 10\ \mu$, $\lambda \leqslant 1\ \mu$, (van de Hulst, 1957) the required scattering function can be described approximately by the following equation (Eiden, 1966):

$$i(\varphi,r,\lambda) = \left(\frac{2\pi r}{\lambda}\right)^2 \times \left[(B(\varphi)+R(\varphi)) + \frac{J_1^2(2\pi r/\lambda)\sin\varphi)}{\sin^2\varphi}\right], \tag{2}$$

where

φ is the scattering angle,
r the particle radius ($r \geqslant 10\,\mu$), and
λ the wavelength of the scattered light;
J_1 $((2\pi r/\lambda)\sin\varphi)$ is the Bessel function of first kind and first order,

$R(\varphi) = \frac{1}{8}[a_1^2(\varphi) + a_2^2(\varphi)]$ and

$B(\varphi) = \frac{3}{8}[(1-a_1^2(\varphi))^2 + (1-a_2^2(\varphi))^2]\dfrac{\sin(3\varphi)}{\sin\varphi}$ with

$a_1(\varphi) = \dfrac{\sin^2[\arccos(1/m_D)-\varphi/2]}{\sin^2[\arccos(1/m_D)+\varphi/2]}$ and

$a_2(\varphi) = \dfrac{\mathrm{tg}^2[\arccos(1/m_D)-\varphi/2]}{\mathrm{tg}^2[\arccos(1/m_D)+\varphi/2]}$;

m_D is the refractive index of the individual particle.

The radiant intensity of the radiation scattered by an individual particle is given by

$$I(\varphi,r,\lambda) = E(\lambda)\frac{\lambda^2}{4\pi^2} i(\varphi,\lambda,r), \tag{2a}$$

with $E(\lambda)$ being the irradiance of the incident light.

According to the nature of the particles suspended in the atmosphere (Eiden, 1966; Volz, 1956), a uniform refractive index $m_D = 1.5$ has been assumed for all aerosol particles.

The term $J_1^2((2\pi r/\lambda)\sin\varphi)\sin^{-2}\varphi$ of eq. (2), which takes into account the diffraction of light by the particle, does not depend on m_D. With increasing r this term becomes more and more important for the process of forward scattering. Thus the scattering processes become more and more independent of the refractive index m_D of the particles.

The analytical relation between the sky radiation and the optical atmospheric quantities is simplest in the solar almucantar; in this case the equation of sky radiation can be written

$$B(\lambda_m) = E_0(\lambda_m) M e^{-\tau(\lambda) M b_x/b_N} (b_x/b_N) f(\varphi,\lambda). \tag{3}$$

$B(\lambda_m)$ is the spectral radiance of the sky observed from an observation site in the pressure level b_x. In this paper, $B(\lambda_m)$ refers to a spectral half width $\Delta\lambda = 100$ Å and a mean wavelength λ_m. The extraterrestrial spectral irradiance of the sun is $E_0(\lambda_m)$.

m is the optical air mass of the point of observation in the sky ($m = \sec z$),
M the optical air mass of the sun ($M = \sec Z$),
z the zenith distance of the point of observation in the sky,
Z the zenith distance of the sun,
b_N the pressure at sea level,

$$f(\varphi,\lambda) = f_D(\varphi,\lambda) + f_R(\varphi,\lambda) = \int_{h=0}^{h=\infty}\int_{r=r_1}^{r=r_2} \frac{\lambda^2}{4\pi^2} i(\varphi,\lambda,r)\, dN_D\, dh + \tau_R(\lambda) \times \frac{3}{16\pi}(1+\cos^2\varphi)$$

is called the scattering function of the turbid atmosphere; it depends on the aerosol size distribution.

Theoretical and experimental investigations can be based upon equation (3) without loosing any essential information about atmospheric aerosol particles.

Moreover, Möller (1954) and Spänkuch (1965) proved that the sky radiation in the solar almucantar is independent of an eventual stratification of the turbid atmosphere.

Absorption effects by aerosol particles or in the region of the wings of the absorption bands of the atmospheric gases are not taken into consideration. The amount of this absorption is not known. However, if the actual scattering processes in the atmosphere are really affected by absorption, its neglect results in an erroneous theoretical interpretation of the measurements as follows: (1) The measured optical thickness of the atmosphere which is increased by absorption, simulates too high values of aerosol number density, (2) The sky radiation which undergoes attenuation by absorption, simulates too small values of aerosol number density.

To derive eq. (3), the sun is assumed to be a point source at an infinite distance. An estimation proves that the error which arises from this idealization, can be neglected for scattering angles $\varphi \geq 1°$ and aerosol size distributions with exponent $\nu^* \geq 2.5$.[1]

Influence of the scattering of higher order and of the albedo of the earth

The theory of primary scattering is based on the assumption that the individual particle scatters only primary solar radiation in direction to the observer. The neglect of the scattering of higher order and the albedo results in a decrease in scattered radiation. Supposing the same optical thickness of the atmosphere, the sky which refers to the primary scattering only, is darker than the real sky which is brightened by all types of scattering processes. However, in the area of the solar aureole, the influence of the scattering of higher order is so small that it can be neglected. But the mathematical approach to the numerical proof of this guess is very difficult. The first author who gave a general estimation of the influence of the scattering of higher order by aerosols was de Bary (1964). This estimation shows that the portion of the scattering of higher order in the solar almucantar decreases towards the sun. The amount of radiance due to the scattering of higher order is almost the same for all scattering angles, but close to the sun, it becomes small compared with the amount of radiance due to primary scattering by aerosol particles.

The aerosol particles favor the forward scattering at small scattering angles. This does not mean a general neglect of the scattering of higher order within the range of small scattering angles $\varphi = 1°–10°$ which is of interest for this paper. The estimation of de Bary shows in the adverse though frequent case:

[1] A paper dealing with this estimation is in preparation.

Table 1. *Turbidity factor $T(\lambda)$ at a constant optical thickness $\tau_D(\lambda)$ of the atmosphere for various λ and ν^**

$\tau_D(\lambda)$	$T(\lambda)$	$\lambda[\mu]$	ν^*
0.35	4.0	0.45	3
	4.5	0.55	3
	3.5	0.45	4
	4.5	0.55	4
0.82	8.0	0.45	3
	9.0	0.55	3
	6.5	0.45	4
	9.0	0.55	4

$\lambda = 0.55\ \mu$; $\nu^* = 4$; $T = 4$, a relative error of about 20 %.

The previous estimation equates the contributions of the scattering of higher order due to aerosol particles and due to Rayleigh particles, in the case of equal extinction. But this must result in an overestimation of the scattering of higher order, at least for small scattering angles. The latter can be shown according to Bugnolo (1960) by means of the theory of probability.

If the upper limit of probability for taking the relevant scattering of higher order into account is set 5 %, the calculation can be based upon mere primary scattering up to $\tau_D(\lambda) = 0.35$. The secondary scattering has to be taken into account for $\tau_D(\lambda) > 0.35$ and the triplicate scattering for $\tau_D(\lambda) > 0.82$. This is valid only for forward scattering. No comments can be given on the scattering processes at greater distances from the sun.

It can be seen from Table 1 that in case of a turbidity $T(0.55\ \mu) \leq 4.5$ the probability for the occurrence of scattering of higher order on aerosol particles is small (≤ 5 %). Therefore, it is admissible at a smaller turbidity to base the calculations for aerosol particles on primary scattering only. The augmentation according to de Bary's estimation is too great and can be diminished by the factor $1/T(\lambda)$ close to the sun. This means the error due to the primary scattering theory in the above example is less than 5 %, and thus within the given accuracy of measurement. On account of this probability consideration, the scattering of higher order can be neglected in an aerosol atmosphere for scattering angles $\varphi = 0°–10°$ and $T(0.55\ \mu) \leq 4.5$. Then, the main contribution to the scattering of higher order comes from the Rayleigh atmosphere. This makes itself felt only at a low turbidity, because then the primary scattering portion of the aerosol atmosphere has grown small.

It is more difficult to estimate the influence of the albedo of the earth. In case of an ideal diffuse Lambert albedo and pure Rayleigh atmosphere, the absolute increase of sky radiation in the solar almucantar is constant for all scattering angles (Sekera *et al.*, 1960). The absolute increase is smaller towards the zenith and greater towards the horizon. The percentage increase is smallest in the immediate neighborhood of the sun and increases with increasing scattering angles, similar to the scattering of higher order. Its maximum amount equals the numerical value of the albedo.

In the presence of aerosol particles in the atmosphere, the scattered radiation in the area of the solar aureole increases very much due to the marked forward scattering. At the same time, the influence of the albedo diminishes because of the relatively small backward scattering. The influence of a small diffuse albedo on the sky radiation can be neglected, e.g. this is valid for Mainz and its surroundings with an average spectral albedo $A = 5\%–10\%$ (Dirmhirn, 1964). The strong albedo over ice and snowfields cannot be neglected any more, the more as the albedo is no longer diffuse. Own observations on the Jungfraujoch in the Alps have shown that there the albedo highly exhibits Fresnel character, which had to be taken into account for the interpretation of these measurements.

Recent investigations have proved that also other surfaces besides snowfields have no Lambert albedo, e.g. sand regions and cloud banks (Bullrich & Eiden, 1964).

Besides the theory of primary scattering, an approximation which had been developed by Deirmendjian (1959) especially for the solar aureole, appeared to be appropriate. This theory has the advantage that it takes into account the scattering of higher order by the atmospheric molecules. However, tabulations of the calculated radiance of the solar aureole according to the theory of primary scattering are readily available for various aerosol size distributions, turbidity factors and solar elevations (Bullrich, 1965). Moreover, they are fit for an extension and adjustment to actual problems. Whereas only a few samples of calculations are accessible which are based upon Deirmendjian's theory.

Influence of an exponential aerosol size distribution with constant and nonconstant exponent

Fig. 2 presents examples of the computed radiance $B(\lambda_m)$ of the solar aureole as a function of the scattering angle φ for a constant turbidity $T(0.55\ \mu) = 2$, a constant zenith distance of the sun $Z = 60°$ and 4 different wavelengths. The boundaries of the size distribution are fixed: $r_1 = 0.04\ \mu$ and $r_2 = 10\ \mu$; the parameter ν^* varies. The following general conclusions can be drawn from this presentation.

(*a*) The radiance of the sky increases towards the sun with decreasing scattering angle φ. This increase depends on ν^*. It is smallest for $\nu^* = 4$ and rise considerably with decreasing ν^*.

(*b*) The distance between the individual spectral curves of the radiance $B(\lambda_m)$ also depends on ν^*. It is largest for $\nu^* = 4$ and diminishes with decreasing ν^*. The effect on the radiance is less in the blue than in the red portion of the spectrum.

The behavior of $B(\lambda_m)$, which has been described under (*a*) and (*b*) can be explained essentially from the scattering function $f(\varphi, \lambda)$, i.e. from the scattering properties of the individual particles and the numerical weighting of the particles within the aerosol size distribution. A decrease in ν^* means that in case of constant turbidity $T(0.55\ \mu)$, the number of large particles increases at the expenses of the small ones. This increases the portion of the forward scattering within the total scattering of a scattering volume or the atmosphere resp. The consequence is an increase of radiance of the sky around the sun.

The greater weighting of the large particles at a smaller ν^* also diminishes the wavelength dependency of the scattered radiation. For pure molecular scattering the wavelength dependency is proportional to λ^{-4}, however, it diminishes in the presence of aerosol particles and with decreasing ν^*. In the case of scattering in a pure aerosol atmosphere, it is proportional to λ^{-1} (Bullrich *et al.*, 1952) at $\nu^* = 3$, and at $\nu^* = 2.5$ the exponent becomes less than 1.

The previous remarks refer to an undisturbed exponential aerosol size distribution with $\nu^*(r)$ = constant. Deviations from such a size distribu-

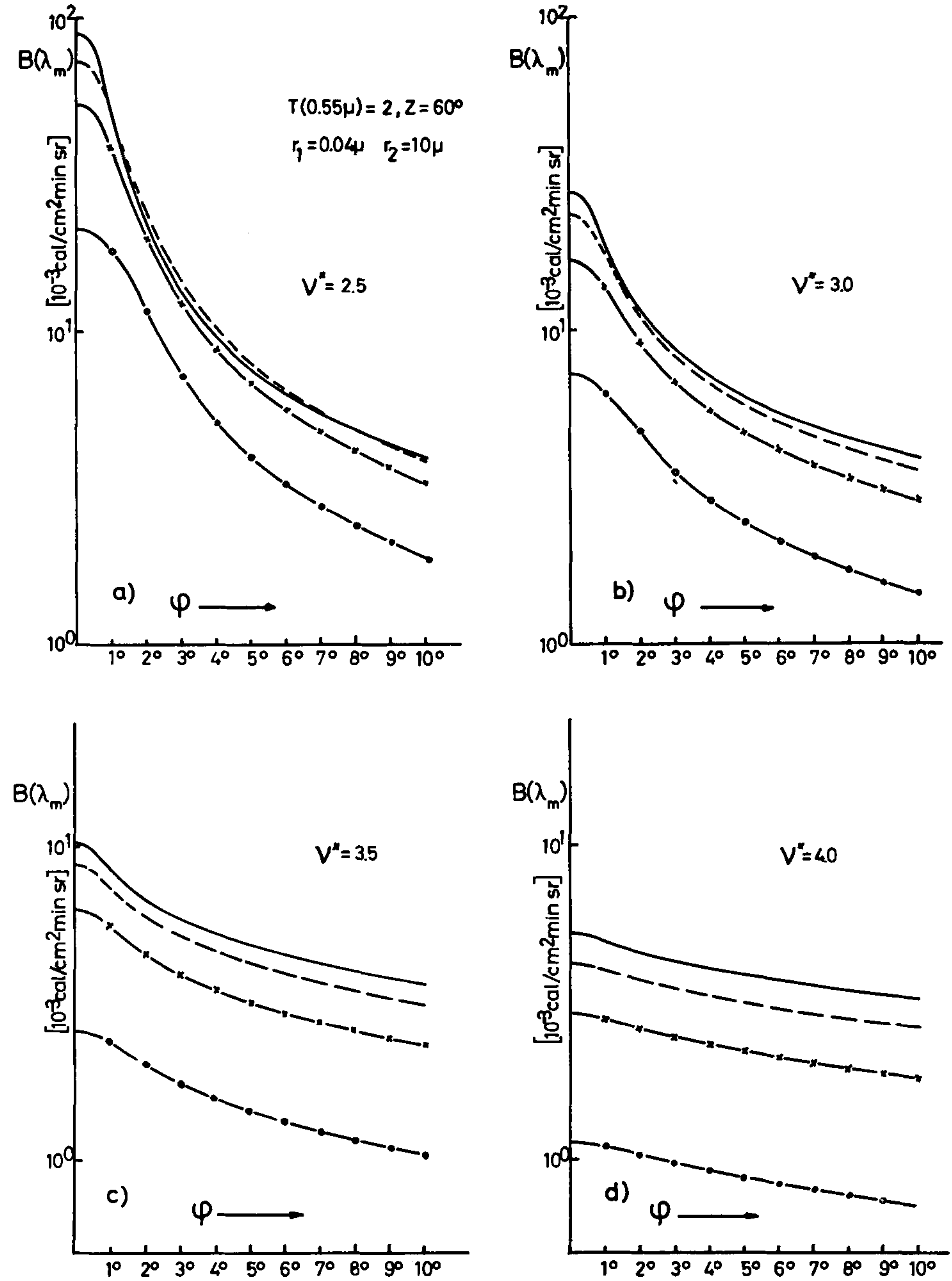

Fig. 2. Theoretical values of the spectral radiance $B(\lambda_m)$ of the solar aureole in the solar almucantar at sea level versus scattering angle φ. Turbidity factor $T(0.55\ \mu) = 2$, zenith distance of the sun $Z = 60°$. —— λ_m, 0.450 μ; – – – λ_m, 0.550 μ; ×—× λ_m, 0.650 μ; ○—○ λ_m, 0.850 μ.

tion must be expected in an polluted atmosphere.

The physical explanation for a part of the measurements (p. 390) could be given only after changing the original model of the turbid atmosphere. The exponent ν^* which had been assumed to be constant, was to be replaced by an exponent which depends on the particle

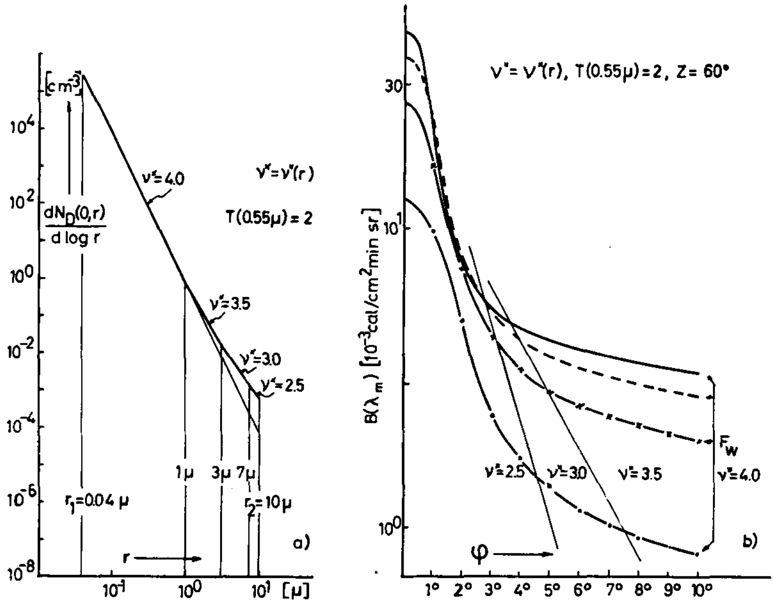

Fig. 3. (*a*) Model size distribution of atmospheric aerosol particles at sea level. Exponent ν^* depending on particle radius r, $\nu^* = \nu^*(r)$. (*b*) Theoretical values of spectral radiance of the solar aureole in the solar almucantar at sea level versus scattering angle φ based on the aerosol size distribution represented in (*a*). Wavelength representation same as in Fig. 2.

radius $r: \nu^* = \nu^*(r)$. For simplifying the computation, the aerosol size distribution was assumed to consist of several sections with constant exponents ν^*. Thus, the computation of the resulting sky radiation could be based on the calculations of Bullrich *et al.*

Fig. 3*a* shows an aerosol size distribution with $\nu^* = \nu^*(r)$, $\nu^*(r') \geqslant \nu^*(r'')$ for $r' \leqslant r''$. The main portion of the particles with $r < 1$ μ is represented by $\nu^*(0.04\ \mu\text{–}1\ \mu) = 4$. From $\nu^*(1\text{–}3\ \mu) = 3.5$ and $\nu^*(3\text{–}7\ \mu) = 3$, it flattens up to $\nu^*(7\text{–}10\ \mu) = 2.5$. The resulting turbidity factor is $T(0.55\ \mu) = 2$, the same as in the Fig. 2*a–d*.

The resulting radiance distribution in the solar almucantar is plotted in Fig. 3*b*; it refers to a zenith distance of the sun $Z = 60°$. The comparison with the relevant graphs 2*a–d* shows that at a scattering angle $\varphi = 10°$, the influence of the size distribution for aerosol particles $r < 1$ μ predominates. The color ratio F_w at $\varphi = 10°$ corresponds to a size distribution with $r_1 = 0.04$ μ, $r_2 = 10$ μ and a constant exponent $\nu^* = 4$. The color ratio is defined as the ratio of the radiance $B(\lambda_m)$ of any spectral range λ_m to the radiance $B(0.55\mu)$ at $\lambda_m = 0.55$ μ, i.e. $F_w = B(\lambda_m)/B(0.55\ \mu)$.

The absolute values of radiance only increased slightly due to the upward bending of the aerosol size distribution.

With decreasing scattering angle φ, the variation of the exponent of size distribution also changes the slope of the curves. The increase of particles with $r > 1$ μ in the atmosphere with regard to the undisturbed distribution with $\nu^* = 4$, effects a gradual steepening of the curves. This mainly turns out in the long wave spectral range. To characterize this behavior, specific zones of the curves in Fig. 3*b* have been marked with a constant ν^*. The increase of the radiance with decreasing scattering angle φ within these zones is equal to the increase due to an aerosol size distribution with a constant ν^* of the same numerical value. With decreasing scattering angles φ the value of ν^* which characterizes the individual zones of the radiance distribution (Fig. 3*b*) decreases too.

An aerosol size distribution which is curved towards smaller particle numbers densities with $\nu^*(r') \leqslant r^*(r'')$ for $r' \leqslant r''$ causes the opposite effects. The absolute values at $\varphi = 10°$ diminish slightly, the shape of the curves flattens, whereas the color ratio is still determined by the aerosol size distribution of the particles $r < 1$ μ.

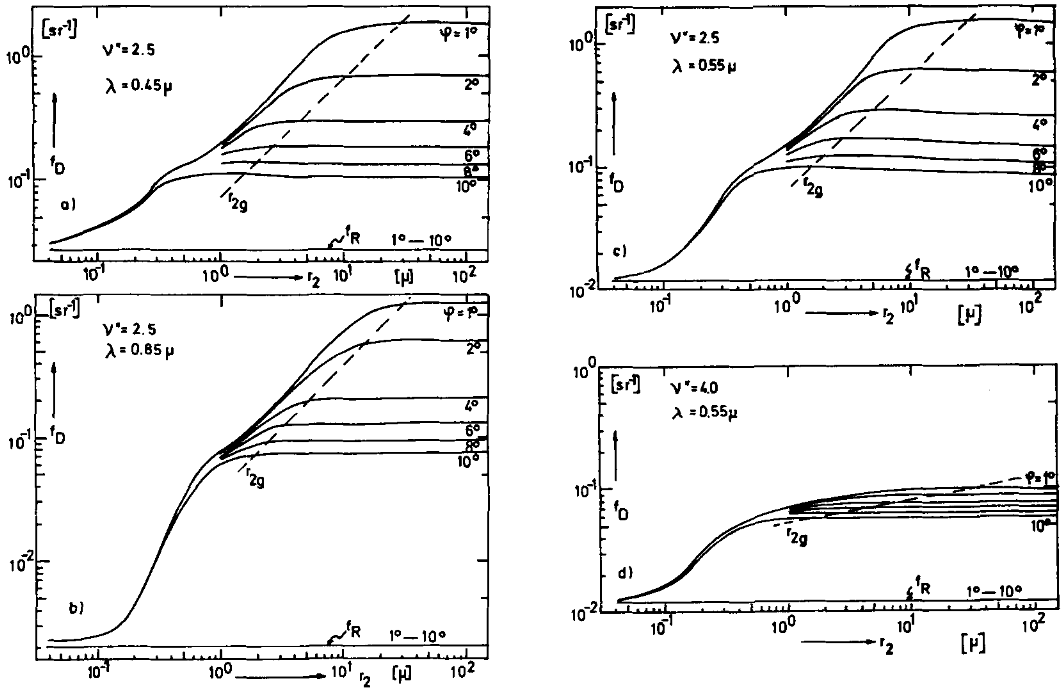

Fig. 4. The sacttering function $f_D(\varphi, \lambda)$ of the aerosol atmosphere as a function of the upper limiting particle radius r_2. Lower limiting particle radius $r_1 = 0.04\ \mu$. T $(0.55\ \mu) = 2$. The dotted line connects the saturation values of $f_D(\varphi, \lambda)$ depending on scattering angle. (*a*) λ, 0.45 μ; ν^*, 2.5. (*b*) λ, 0.85 μ; ν^*, 2.5. (*c*) λ, 0.55 μ; ν^*, 2.5. (*d*) λ, 0.55 μ; $\nu^* = 4.0$.

Influence of the limits of the aerosol size distribution

According to eq. (3) the sky radiation mainly depends on the aerosol size distribution and the limiting radii by the scattering function $f(\varphi, \lambda)$. The remainder of eq. (3) is influenced by the aerosol size distribution and thus by the limiting radii only by the optical thickness $\tau(\lambda)$ of the atmosphere. In case of a constant turbidity factor $T(0.55\ \mu)$ the variation of $\tau(\lambda) = \tau_R(\lambda)\, T(\lambda)$ is negligible with a variation of the lower limiting radius r_1 between 0.04 μ and 0.08 μ and of the upper limiting radius r_2 between 1.0 μ and 150 μ. This is valid for the spectral range of interest from $\lambda = 0.45\ \mu$ through $\lambda = 0.85\ \mu$ and the exponents of the aerosol size distribution $\nu^* = 2.5$ through 4.0.

It can be proved theoretically that the scattering function $f(\varphi, \lambda)$ is also hardly influenced by a variation of the lower limiting radius r_1 between 0.04 μ and 0.08 μ. It is therefore admissible to treat the scattering function as a function of the upper limiting radius r_2 only i.e. $f(\varphi, \lambda) = f(r_2)$.

The components $f_D(\varphi, \lambda)$ and $f_R(\varphi, \lambda)$ of the scattering function $f(\varphi, \lambda)$ are plotted in Fig. 4*a*–*d* as functions of the upper limiting radius r_2 for $T(0.55\ \mu) = 2$. Fig. 4*a* shows $f_D(r_2)$ for an aerosol size distribution with $\nu^* = 2.5$ and the wavelength $\lambda = 0.45\ \mu$. The parameter of the curves is the scattering angle φ. Fig. 4*b* represents the same set of curves, however, for the wavelength $\lambda = 0.85\ \mu$. The Figs. 4*c* and 4*d* refer to the wavelength $\lambda = 0.55\ \mu$ and to an aerosol size distribution with $\nu^* = 2.5$ and $\nu^* = 4.0$ resp.

The scattering function $f_R(\varphi, \lambda)$ of the molecular atmosphere does not depend on the limiting radii of the aerosol size distribution. It has been plotted to demonstrate the greater weighting of the scattering function of the aerosol atmosphere depending on r_2, within the total scattering function $f(\varphi, \lambda)$.

The change of $f_R(\varphi, \lambda)$ within the range of scattering angle $\varphi = 1°$–$10°$ is smaller than the drafting accuracy.

All the scattering functions of the turbid atmosphere which have been plotted in Fig.

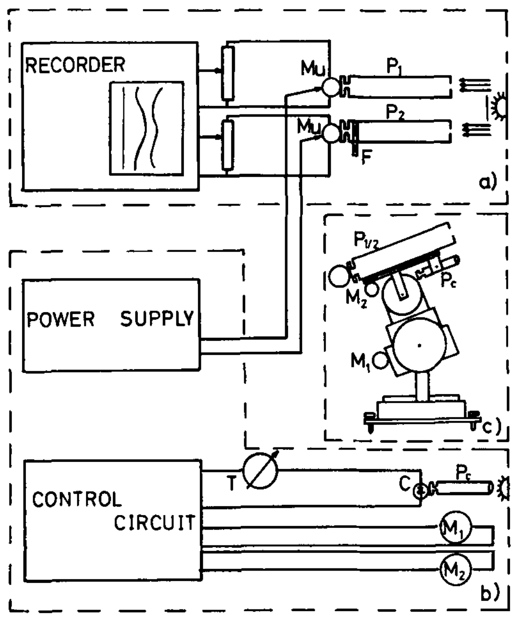

Fig. 5. Schematic of the solar aureole photometer. (*a*) Photoelectric measuring system. *Mu*, photomultiplier; P_1, photometertube to controle atmospheric turbidity with one interference filter; P_2, photometertube with filterdisk *F*. (*b*) Control circuit for scanning motor M_2 and auxiliary photometer P_C. *C*, photodiode; *T*, indicator instrument for turbidity factor. Regulated power supply for photomultiplier *Mu* and sun follower motor M_1. (*c*) Parallactic mounted photometer tubes.

4*a–d* show the same characteristic trend as functions of r_2. In the beginning, $f_D(r_2)$ increases rapidly, but with increasing r_2 it converges to a saturation value. The radius r_{2g} that denotes the beginning of saturation of the scattering function $f_D(r_2)$ depends only on the scattering angle φ. The broken curves in the Fig. 4*a–d* demonstrate the dependence of the saturation radius r_{2g} on the scattering angle φ. This saturation radius is $r_{2g} = 1.5\ \mu$ at $\varphi = 10°$; with decreasing scattering angle φ, it is shifted to larger values and it reaches its maximum of $r_{2g} = 30\ \mu$ at $\varphi = 1°$.

Another common feature of the graphs of Fig. 4*a–d* is the great dispersion of the scattering functions by the variation of the parameter φ. This dispersion becomes noticeable at about $r_2 \approx 5\ \mu$.

This implies that from this particle size upwards the forward scattering in the atmosphere becomes more and more marked and distinct. The larger the radius r of the aerosol particle, the smaller the forward lobe of scattered radiation, i.e. the scattered radiation that emerges from a unit volume of air or the whole atmosphere, is noticeably influenced by large particles only within a narrow scattering angle range $0 \leqslant \varphi \leqslant \varphi_0$. This scattering angle range $(0 \leqslant \varphi \leqslant \varphi_0)$ becomes gradually narrower with increasing particle radius. This scattering property of the particles explains the fact that the scattering function of the aerosol atmosphere does not exceed a fixed saturation value, even if the limiting radius r_2 continues growing. Moreover, this property explains the shifting of the saturation radius r_{2g} to larger values with decreasing scattering angle.

All these statements are independent on the wavelength chosen and the exponent ν^* of the aerosol size distribution. The latter variables cause only quantitative changes of the scattering function $f_D(r_2)$.

The relative increase of $f_D(r_2)$ with increasing r_2 is more important for long than for short wavelengths (Fig. 4*a* and *b*). An increase of the exponent ν^* of the aerosol size distribution effects a decrease of dispersion of $f_D(r_2)$ with the scattering angle φ (Fig. 4*c* and *d*).

A change in turbidity $T(0.55\ \mu)$ causes a shifting of the entire set of curves parallel to the ordinate.

Hence it can be seen that just the study of the forward scattering gives new information on the properties of large and giant particles. On the other hand, it can be seen that this information is limited. In case of a normal turbid atmosphere the analysis of the circumsolar radiation only can reveal particles of the size range $r_1 < r \leqslant 30\ \mu$.

Apparatus

The radiance of the solar aureole has been measured with a special photoelectric photometer of own design (Fig. 5). The main features of this apparatus are:

1. The measured sky radiation is read in absolute radiometric units, i.e. in units of radiance [cal/cm² min sr]. The calibration is based upon a radiation standard on his side calibrated by the Federal Bureau of Standards (Physikalisch-Technische Bundesanstalt, calibration certificate No. 8323-PTB-62). The calibration has been repeated after each of the

measuring series in order to eliminate any errors due to a change in the operating parameters of the instrument by switching it on or off.

The maximum relative error of the measured absolute radiance amounts to 15 %. It consists of the relative error of the radiation standard of 5 %, the temperature error of the receiver of 4.0 %, a spectral inaccuracy of the combination receiver—interference filter of 3.5 %, the influence of stray light of the apparatus of 1 %, inaccuracies of the mechanical structure of the photometer tube of 1 %, and the error in reading of 0.5 %.

2. The spectral sensitivity of the photoelectric receiver in connection with 5 narrow band interference filters guarantees a satisfactory spectral resolution of the sky radiation in the visible and near infrared portion of the electromagnetic spectrum.

The receiver used is a photo multiplier with S_1 photo cathode (Maurer Vp 11 Ad.)

The spectral centers of the filter range of the interference filters are $\lambda_m = 0.448\ \mu$, $\lambda_m = 0.544\ \mu$, $\lambda_m = 0.621\ \mu$, $\lambda_m = 0.709\ \mu$ and $\lambda_m = 0.847\ \mu$. Their average half-width is $\Delta\lambda = 0.013\ \mu$. These filter ranges have been selected to measure the sky radiation within the spectral range in question at almost equidistant intervals. Simultaneously it had to be kept in mind not to select filter ranges which coincided with the absorption bands of the atmospheric gases. The only exception is the Chappuis band of ozone from $\lambda = 0.44\ \mu$ through $0.65\ \mu$ in the visible; it could not be evaded.

3. The photometer is qualified for continuous operation and adapted to field work. The measuring tube is parallacticly mounted and follows automaticly the sun. Simultaneously this tube scans the sky above the sun and tangential to the ecliptic. Thus the distribution of sky radiance is measured continuously from $\varphi = 1°$ through $\varphi = \pm 15°$.

It takes 10 minutes to perform one measuring set of the spectral radiance distribution. During this time interval the optical air mass of the points of observation in the sky changes due to the propagation of the sun, however. In temperate latitudes, this effect can be neglected. To control the variation of the atmospheric turbidity during the measuring time the sky radiation in one wavelength range ($\lambda_m = 0.544\ \mu$) is measured by a second parallel mounted photometer tube (Fig. 5).

Without structural changes, this photometer can also be operated in an azimuthal mounting.

4. The parasitic stray light of the apparatus is small compared with the sky radiation even if it is measured in the immediate circumsolar area. The photometer tubes are constructed without using lenses or reflector systems. Scratches on the surfaces of the lenses or reflectors, bubbles or any other inhomogeneities effect, due to the great values of circumsolar radiance, unpredictable errors of the measurements.

The path of rays within the photometer tube only depends on the arrangement and the dimensions of the circular diaphragms, which have been carefully produced of stainless steel. The field of view that results from the ratio of the diameter of the diaphragm to their distance, is $\beta = 0.5°$. Thus, it is possible to measure the sky radiation at 1° from the center of the sun with a safety distance of 0.25° from the sun's limb.

To suppress the stray light, the photometer tube has been designed with a large diameter compared with the diaphragm aperture. Moreover, it is lined with black velvet and equipped with additional diaphragms. The last diaphragm has a conical shape with a 45° inclination and is mirrorfinished towards the interior of the tube. In this way it is possible to define exactly the reflection of the radiation that passes by the aperture of the last diaphragm. It is scattered into the area behind the diaphragm. The interference filters are fixed near the end of the tube where they are protected from contamination.

Unavoidable diffraction processes at the entry diaphragm also effect errors of the measurements.

In order to avoid this complication, two external light stops have been mounted in such a way that the entry diaphragm of the photometer tube was shaded, the field of view, however, was not reduced. By these means, the stray light of the apparatus is limited to less than 1 % of the measured sky light.

5. The turbidity factor T is measured by an auxiliary photometer with photoresistor whose spectral response is controlled by interference filters of the wavelengths $\lambda_m = 0.448\ \mu$, $\lambda_m = 0.544\ \mu$, $\lambda_m = 0.621\ \mu$ and $\lambda_m = 0.709\ \mu$ with the average half-width $\Delta\lambda = 0.013\ \mu$.

The auxiliary photometer is also used to *control the exact focussing or tracking of the* apparatus resp. It is continuously directed towards the sun during the operation. In this way the phototubes can be focussed with regard to the sun with an accuracy of 0.1°.

Measurements

Observations sites

Measurements of the solar aureole have been taken at 3 different observation sites with different atmospheric turbidity conditions.

The stations are:

(*a*) Mainz, Germany, (*b*) the research station Jungfraujoch in the High Alps, Switzerland, (*c*) the Haleakala Observatory on the island of Maui, Hawaii.

(*a*) The station in Mainz is located at 50° N and 08°16′ E on a tower of the university to the west of the city 140 m above MSL. The turbidity of the atmosphere is mainly effected by pollution. In case of fair weather, it can hardly be expected to have a natural undisturbed turbid atmosphere. The industrial smoke production in the Rhine Main basin causes considerable concentration of aerosol particles in the lowest 100–200 meters. Especially during inversion situations in fall and winter the aerosol atmosphere is characterized by a sharp discontinuity.

The albedo is mainly influenced by the suburban fields and meadows and may be assumed to be 5–10 % in the visible (Dirmhirn, 1964). At this station, measurements were taken from August thru September 1964.

(*b*) The measurements at the research station Jungfraujoch in the High Alps have been taken at the Sphinx Observatory. This observation site is located at 46°33′ *N* and 07°59′ E 3570 m above MSL. Here it can be expected to find a natural continental turbid atmosphere due to the height of the station as well as to the relatively large distance from industrial areas This means that the turbidity of the atmosphere is due to aerosol particles which have been formed in the atmosphere and at the surface of the lithosphere, without human influence.

Since the station is located above the Aletsch glacier, which is here directed towards SSE, amid snow covered mountain slopes, a high albedo of 80–90 % must be assumed (Dirmhirn, 1964).

Measurements were taken here from the beginning to the end of November 1964.

(*c*) The third observation site, the Haleakala Observatory, is the Sun and Airglow Observatory of the Hawaii Institute of Geophysics (University of Hawaii) on the island Maui, Hawaii. The observatory is located on top of the extinct volcano Haleakala at 20°43′ N and 156°15′ W, 3050 m above MSL. The station is situated within the region of the subtropical trade wind system above the undisturbed trade wind inversion and the trade wind cumulus layer.

Due to the optimal distance from the continents, this observation site guarantees a most undisturbed maritime atmosphere.

During the period of record from 1 August through 15 September 1965, the trade wind cumulus layer has been only imperfectly developed. The cloud cover came to 2/10–3/10 so that at a high solar elevation, the dark water surface of the Pacific prevailed. The albedo has to be assumed to amount to 20–30 %.

Discussion of the results

The total of the measurements obtained is too voluminous for being presented in this paper. Therefore, selected measurements, characteristic of the individual observation sites, are presented and discussed.

1. POLLUTED TURBID ATMOSPHERE: Measurement taken at Mainz, 28 August 1964.

(*a*) *Local atmospheric conditions:* The observation site has been under the influence of a high pressure cell over Eastern Europe which slowly moved eastward.

Radiation cooling during a cloudless night caused an inversion layer above the Rhine Main basin in an altitude of about 200 m under which the aerosol particles produced in this area accumulated. After sunrise at 05.30 LST, the upper edge of this relatively homogeneous brownish dust layer could be clearly distinguished from the blue clear sky and the surrounding mountain ranges. At this time, the horizontal visibility was about 4 km. The increasing heating of the surface and the beginning of convection dissolved the inversion in the late forenoon and initiated the mixing of the lower troposphere. At 13.00 LST, the horizontal visibility raised up to about 10 km and no haze layer could be recognized any more.

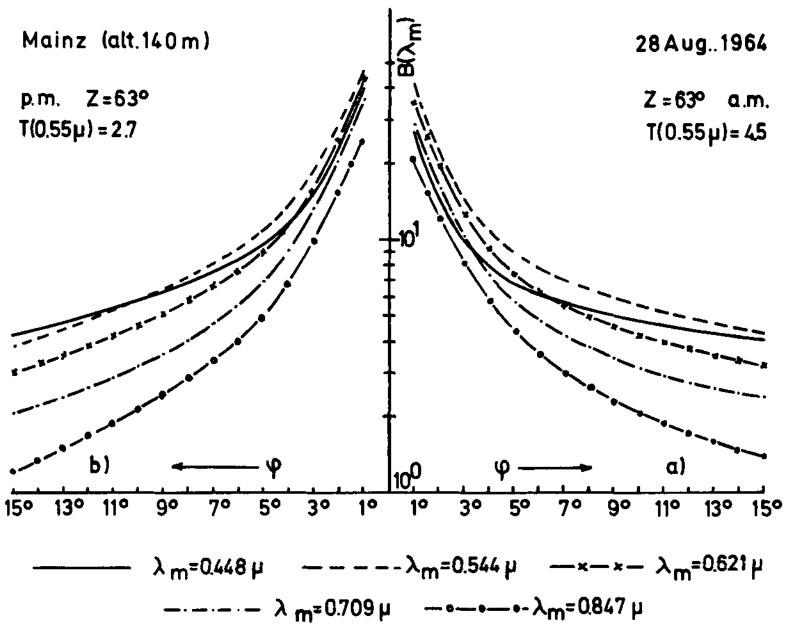

Fig. 6. Measured spectral radiance $B(\lambda_m)$ of the solar aureole in the solar almucantar versus scattering angle φ. 28 Aug 64, Mainz. $B(\lambda_m) = 10^{-3}$ [cal/cm² min sr]. (*a*) 8.30 CET, (*b*) 16.23 CET. CET, Central European Time.

From now the horizontal visibility increased slowly but continuously. This turbidity pattern has been frequently observed and can be taken as a characteristic feature of the measuring period.

The dissolution of the inversion layer and the increase of the horizontal visibility can also be observed in the diurnal variation of the spectral atmospheric turbidity. The turbidity factor changed from $T(0.55\ \mu) \approx 4.5$ in the early morning to $T(0.55\ \mu) \approx 2.5$ in the late afternoon. Almost together with the dissolution of the inversion and the increase of the horizontal visibility, discontinuous decrease of the atmospheric turbidity started. Obviously, the aerosol particles which had been lifted by convection have been carried off by strong upper winds.

(*b*) *Physical interpretation of the measurements:* Fig. 6 represents a forenoon and afternoon set of measurements performed on 28 August 1964. The measured absolute spectral radiance $B(\lambda_m)$ of the solar aureole has been plotted as a function of the scattering angle φ. The curve parameter is the mean wavelength λ_m of the spectral range under consideration. The zenith distance Z of the sun and the measured turbidity factor $T(0.55\ \mu)$, valid for the individual measuring set, are indicated on the graph. To compare the measurements, they are presented in this paper in a symmetric plotting.

The curves show a gradually steepening slope with decreasing scattering angles φ, i.e. towards the sun's limb. The radiance of the blue spectral range ($\lambda_m = 0.448\ \mu$) increases less than that of the green ($\lambda_m = 0.544\ \mu$) and the red ($\lambda_m = 0.621\ \mu$) portion of the spectrum. At the same time, a marked difference in the spectral distribution of the forenoon and the afternoon values of the radiance $B(\lambda_m)$ can be seen.

In order to evaluate the aerosol particle size distribution and concentration, the measured results have been compared with theoretical values. The interpretation of the measurements based on the assumption of aerosol size distributions with constant exponent ν^*, did not lead to any agreement between the measurements and the theory. Nor the variation of the upper boundary radius r_2 give any satisfactory result. Only the assumption of an aerosol size distribution with an exponent ν^* depending on the particle radius r furnished the agreement A detailed analysis of the measurements presented

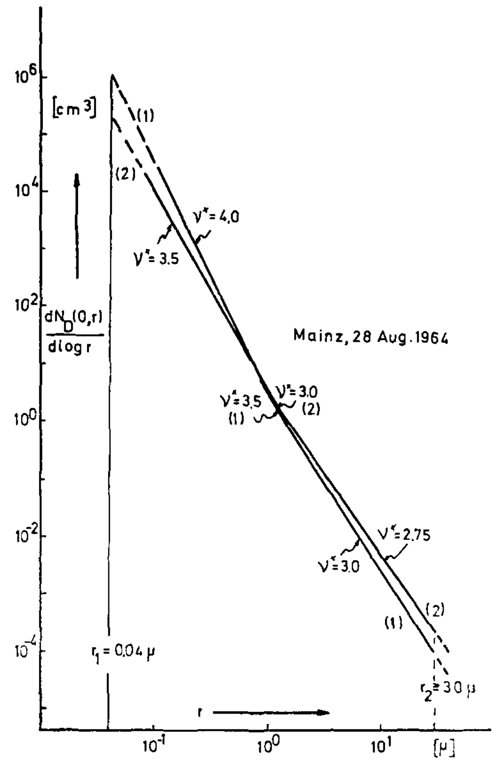

Fig. 7. Aerosol size distribution of the atmosphere. 28 Aug. 64, Mainz. *1*, 8.30 CET; *2*, 16.23 CET.

in Fig. 6 resulted in the size distributions shown in Fig. 7.

This method of comparison does not allow an exact determination of lower boundary radius r_1. A variation of r_1 from 0.04 μ to 0.08 μ effects a change in the absolute values of radiance for φ 10° of about 10 %. Since the measuring accuracy is 15 %, this change cannot be confirmed any more.

In Fig. 7, the upper particle limit has been indicated to be $r_2 \geq 30$ μ. As mentioned previously, this means that this method does not allow to detect larger particles.

Fig. 7 proves, that the decrease of turbidity following the dissolution of the inversion layer has been mainly caused by the convectional lifting and removal of the particles in the size range 0.1 $\mu \leq r \leq 1.0$ μ. The shifting of the exponent of the aerosol size distribution for $r \leq 1$ μ from $\nu^* = 4.0$ in the morning to $\nu^* = 3.5$ in the afternoon appears to indicate that mainly small particles have been removed.

On the other hand, the decrease of the exponent ν^* during this day can also be interpretated as an effect of air pollution due to the smoke of household firing or other sources which is strongest in the morning. Then, it is not necessary to assume that mainly small particles have been removed by the convectional processes. According to Robinson (1962) the typical smoke particles are grouped within the size range 0.5 $\mu \leq r \leq 5$ μ. Thus, the number of atmospheric aerosol particles is augmented only in this limited size range. Consequently, the slope of the complete aerosol size distribution and thus the value of the exponent are decreased.

This interpretation is supported by the measurements, discussed in the next section.

2. Polluted Atmosphere: Measurement taken at Mainz, 2 September 1964.

(*a*) *Local atmospheric conditions:* The general weather situation is charakterized by a strong high of great vertical extent with its center over Central and East Europe. The sky had been cloudless except for some fair weather cumuli over the mountain ranges in the northwest. The wind from ENE blew with a rather constant speed of about 5 m/sec.

The horizontal visibility of about 30 km was extraordinarily good this day. From 12.00 LST thin homogeneous veils of smoke could be recognized in front of the sun, drifting along from a scene of fire east of the observation site. During the passage of the smoke, the solar aureole appeared brighter and larger.

The atmospheric turbidity has not been noticeably affected by this veil of smoke. The measurements showed nearly uniform turbidity conditions, unusual for the Rhine Main area.

(*b*) *Physical interpretation of the measurements:* The Figs. 8*a* and 8*b* show two sets of measurements with equal zenith distance of the sun which have been recorded before and during the visible passage of the smoke.

Obviously, the smoke pollution has caused a considerable increase of the slope of the curve towards smaller scattering angles, i.e. towards the sun. Moreover, marked differences in the spectral distribution of the radiance can be seen. They refer to the blue, the green and the red portion of the spectrum.

Just as in the previous section, the physical interpretation of these measurements requires

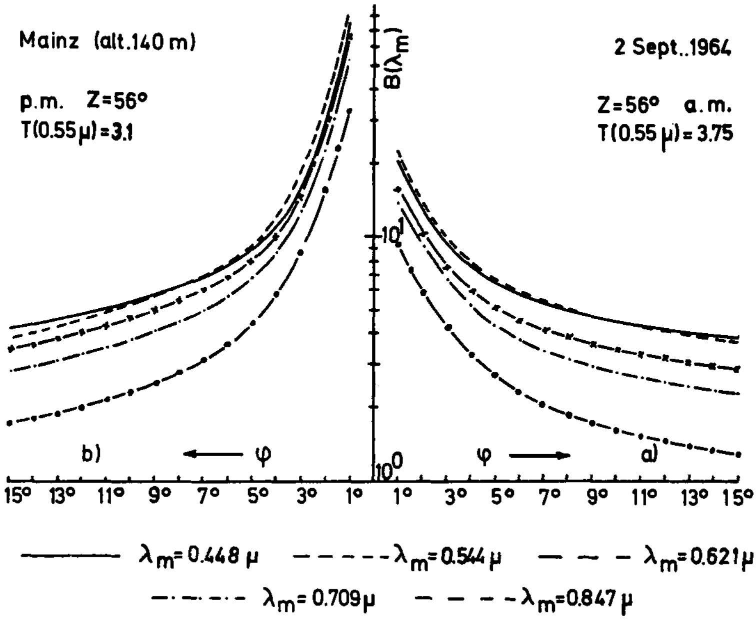

Fig. 8. Same as Fig. 6. 2 Sept. 64, Mainz. (*a*) 9.35 CET, (*b*) 15.30 CET.

the assumption of aerosol size distributions with variable exponents $\nu^*(r)$.

Fig. 9 shows the aerosol size distributions, related with the measurements of radiance influenced by the smoke, Fig. 8*a*, and not influenced by the smoke, Fig. 8*b*. Obviously, the addition of smoke particles causes a flattening of the aerosol size distribution, i.e. a decrease of ν^*.

As mentioned in the previous section, Robinson has found the size of smoke particles between $0.5\ \mu \leqslant r \leqslant 5\ \mu$.

The atmospheric aerosol size distributions presented in Fig. 9 also prove a lower limiting radius of smoke particles of $r_1 = 0.4\ \mu$–$0.5\ \mu$. However, in contrast to Robinson's result, the upper limiting radius is much larger. Before the smoke pollution the upper limiting radius r_2 of the aerosol size distribution has been $r_2 = 10\ \mu$. Its increase implies an upper limiting radius of smoke particles of $r_2 \geqslant 30\ \mu$. The bulk of the smoke particles can be found within the size range $r = 0.6\ \mu$–$1.0\ \mu$.

The existence of the smoke particles and their size distribution give an at least qualitative explanation for the dependence of the exponent ν^* of the aerosol size distribution on the particle radius r.

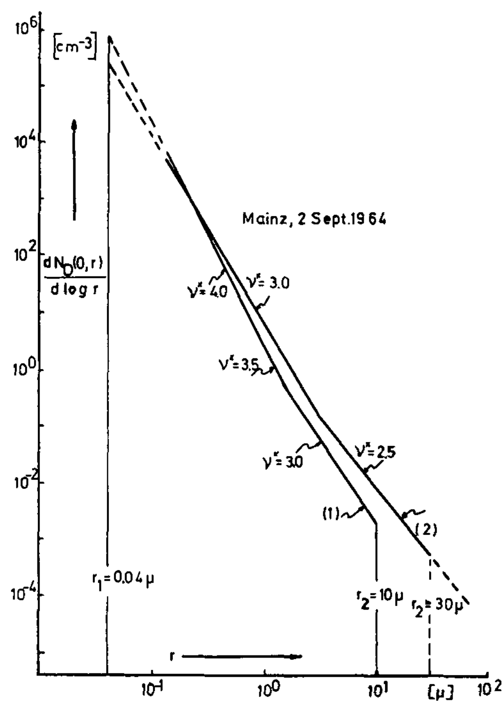

Fig. 9. Same as Fig. 7. 2 Sept. 64, Mainz. *1*, 9.35 CET; *2*, 15.30 CET.

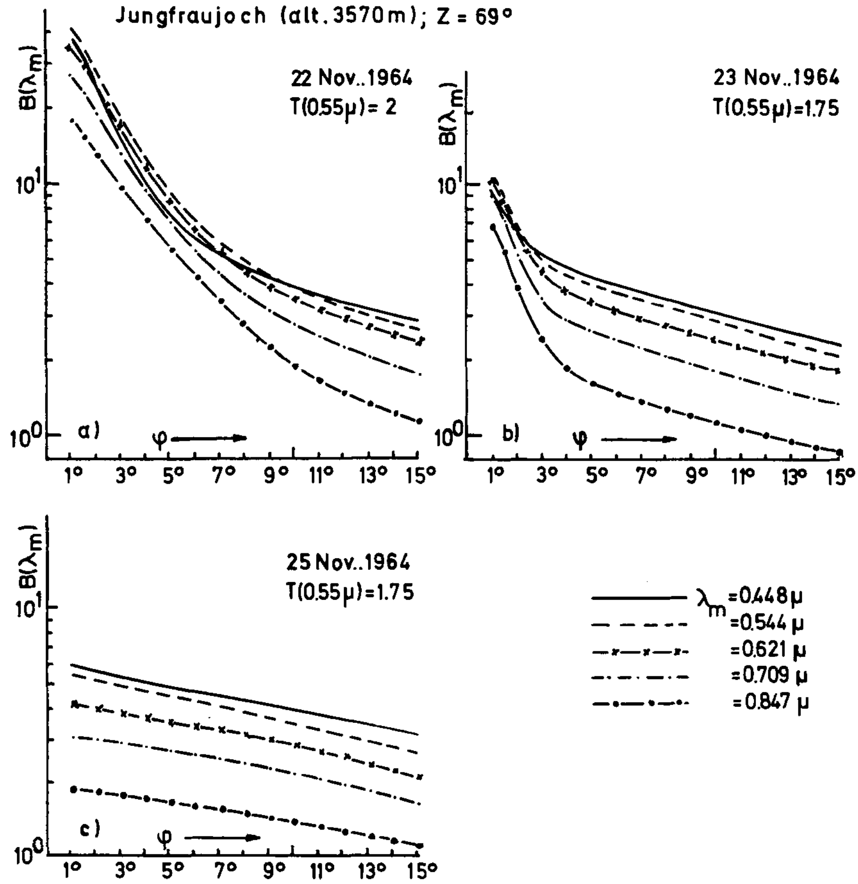

Fig. 10. Same as Fig. 6. Jungfraujoch. (*a*) 22 Nov. 64, (*b*) 23 Nov. 64, (*c*) 25 Nov. 64.

3. *Unpolluted Continental Atmosphere:* Measurements taken at Jungfraujoch, 22–25 November 1964.

(*a*) *Local atmospheric conditions:* The weather situation is charakterized by the influence of a weak cell of high pressure. On 18 and 19 November, the observation site had been passed by a cold front from NE with great cloudiness and heavy precipitation. On 27 November again, the site has come under the influence of a low pressure system which has approached from NW.

During the entire measuring period the horizontal visibility has been continously good amounting to about 150 km (Black Forest and Vosges to be seen).

The diurnal variation of the atmospheric turbidity factor has been small. The daily means show a slight decrease from the beginning of the measuring period up to the 25 November.

(*b*) *Physical interpretation of the measurements:* The Figs. 10*a–c* show 3 measuring sets of the circumsolar sky radiation, taken on three successive days at the same zenith distance of the sun. The individual measurements differ very much; this implies rapid changes of the atmospheric conditions.

A detailed quantitative interpretation of these measurements, however, appears to be impossible without knowing the amount and charakteristic features of the spectral albedo. There is evidence from certain observational facts that no pure Lambert albedo can be assumed. Middleton & Mungall (1952) found, that especially at a low solar elevation, the albedo of snow fields mainly follows Fresnel's law of reflection.

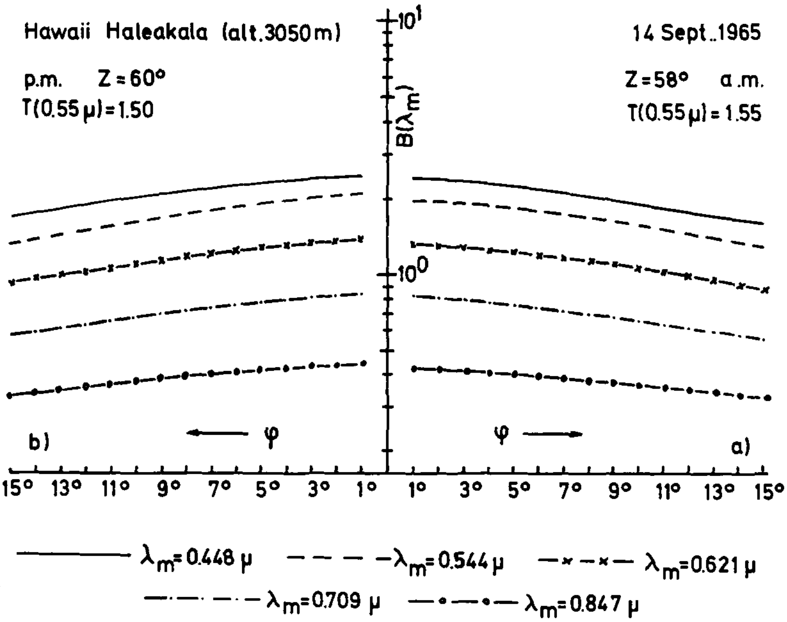

Fig. 11. Same as Fig. 6. 14 Sept. 65, Haleakala, Maui, Hawaii.

In addition the surface of the snow cover plays an important role. It does not only influence the character but also the amount of the albedo. Finally, it is a great handicap that the irregular orography of the environs of the Jungfraujoch does not allow a simple geometric approach for taking the albedo into account. Hence a quantitative interpretation would be too speculative.

However, qualitative conclusions can be drawn from the measurements represented in Fig. 10 as follows:

(1) 22 November 1964: The gradual steepening of the curve towards the sun implies the presence of a relatively great number of particles of $r \geq 1$ μ. The increase for $\varphi < 4°$ implies an upper boundary radius of the particles of $r_2 \cong 10$ μ. The small spectral dispersion of the curves can be explained by an exponent of the aerosol size distribution $\nu^* = 2.5$–3.0.

(2) 23 November 1964: The slope of the curve has decreased, this implies that the number of giant particles ($r \geq 1$ μ) has decreased. At the same time, the dispersion of the individual spectral curves has increased, this implies an increase of the exponent ν^* of the aerosol size distribution.

(3) 25 November 1964: The shape of the curve has become rather flat. This means that the upper boundary radius r_2 has continued shifting towards smaller particles, now being about 3 μ–5 μ. The spread of the spectral curves has almost remained the same, i.e. the exponent of the aerosol particle size distribution which may be assumed to be $\nu^* \cong 4.0$, has not changed.

Obviously, a passage of a front effects, due to the upslide motions connected with it, the transport of a large number of giant aerosol particles into the free atmosphere. Thus, not only the upper limiting radius is shifted towards larger particles, but also the mean aerosol size distribution of the atmosphere above the observation site flattens, i.e. the exponent ν^* becomes smaller. The subsidence in the following high causes an increased sedimentation of the atmospheric aerosols, so that the giant particles are eliminated, the exponent of the aerosol size distribution increases again.

4. Unpolluted Maritime Atmosphere: Measurement taken on Maui, Hawaii, 14 September 1965.

(*a*) *Local atmospheric conditions:* The weather situation not only of this day but also of the entire measuring period is characterized by a weakly or even not at all developed trade wind

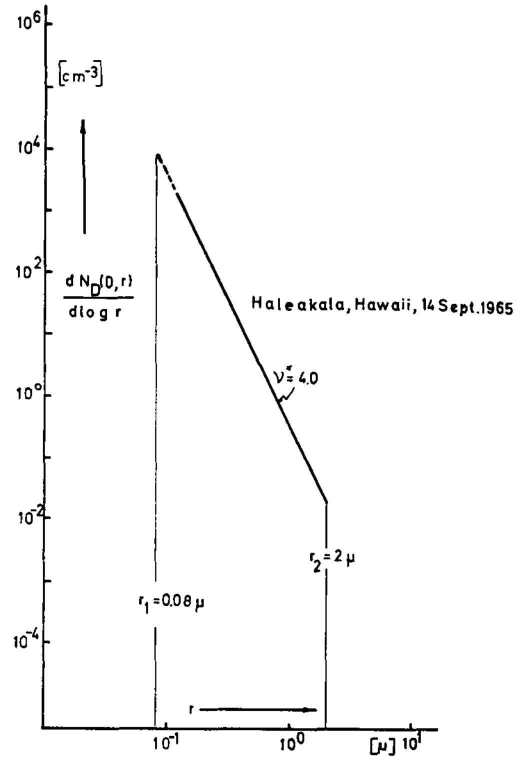

Fig. 12. Same as Fig. 7. 14 Sept. 65, Haleakala, Maui, Hawaii.

circulation. No wind speed more than 5 m/sec has been observed. On 14 September 1965 there has been no noticeable wind during the measurements.

Immediately above the surface of the ocean, a homogeneous dense haze layer could be observed. The horizontal visibility at the observation site has been good surpassing 160 km (Mauna Loa to be seen). This has been true for the entire measuring period with only minor variations.

The measurement of the spectral optical thickness of the atmosphere revealed a marked anomalous atmospheric extinction. In case of "normal" extinction the spectral optical thickness of the aerosol atmosphere $\tau_D(\lambda)$ increases continously with decreasing wavelength λ. If from a certain wavelength (here $\lambda \approx 0.55\ \mu$) the optical thickness starts to decrease; this behavior is called anomalous extinction. On the one hand, this anomalous extinction can be due to the absence of Aitken nuclei (Danzer & Bullrich, 1966). This demands a shifting of the maximum of the aerosol size distribution towards larger particles. On the other hand, the particle number of a narrow size interval may exceed considerably the normal value. This could be explained with the existence of a layer of monodispersive aerosol particles in the lower stratosphere due to the eruption of the volcano Agung on the island of Bali in 1963. However, any clue to this assumption, e.g. Bishop's rings, could not be observed during the measuring period. Nevertheless, in spite of the little turbidity and albedo, the sky appeared whitishblue.

(*b*) *Physical interpretation of the measurements:* Two sets of the forenoon and the afternoon measurements of the solar aureole at the same zenith distance Z of the sun are represented in Fig. 11. The curves have a noticeably flat shape. None of the measurements shows the characteristic steep slope towards small scattering angles which has been found at Mainz.

The comparison of the forenoon and the afternoon measurements does not reveal any difference that is beyond the measuring accuracy.

All the measurements show a mean aerosol size distribution which is independent on the air mass or the time of the day and has a constant exponent $\nu^* = 4.0$ with the limiting radii $r_1 = 0.08\ \mu$ and $r_2 = 2\ \mu$. This size distribution is represented in Fig. 12.

In order to match the measured and the theoretical radiance distributions of the aureole, the anomalous extinction in the spectral range $\lambda_m = 0.448\ \mu$ has to be taken into account. In case of normal extinction, the amount of the radiance of the spectral range under consideration should be greater. But there is coincidence between the theory and the measurement if a turbidity factor is applied which corresponds to the measured turbidity factor $T(0.448\ \mu) \approx 1.15$ ($T(0.621\ \mu) \approx 1.7$, $T(0.709\ \mu) \approx 1.9$).

Thus, the anomalous extinction can also be detected by sky radiation measurements. However, the cause of this anomalous extinction is still an unsolved problem. A qualitative explanation would be the lack of Aitken nuclei which seems to be verified by the measured lower limiting radius $r_1 = 0.08\ \mu$. However, there is an objection insofar as the theoretical increase in radiance $B(\lambda_m)$ due to the shifting of $r_1 = 0.04\ \mu$ to $r_1 = 0.08\ \mu$ for $\varphi = 10°$ is independent of Z and amounts to about 10 %. This effect is too small with regard to the relative error of the measurements of 15 %.

Conclusions

The discussion of the measurements has proved that the spectral radiance distributions of the circumsolar sky radiation and also the aerosol particle size distributions of the atmosphere show characteristic differences at the different observation sites. The basic reason for these differences seems to be the properties of the earth's surface. Apart from the albedo the circumsolar sky radiation is mainly controlled by continental and maritime aerosol sources as well as air pollutions in the near and far surroundings of the observation site.

At Mainz, the sky radiation is noticebly influenced by smoke particles from household and industrial firings. The air pollution seems to be also the reason for the dependence of the exponent ν^* of the measured aerosol size distribution on the radius r of the aerosol particles.

At Mainz, no changes in the circumsolar radiance distribution could be observed which are due to large scale changes in synoptic air mass. Because of the considerable air pollution, these processes have no effect on the atmospheric aerosol size distribution.

The research station Jungfraujoch in the High Alps is unaffected by the immediate influence of air pollution due to its height and great distance from industrial areas; here, changes in the air mass influencing the atmospheric aerosol size distribution can be observed. But no quantitative interpretation of the measurements can be given due to the high and unknown albedo.

During the period of record in Hawaii, the measurements did not reveal any immediate influence of the surface nor of large scale air mass transport on the sky radiation. The analysis of these measurements has shown the smallest particle concentration with the smallest upper boundary radius r_2. Spectral distribution and absolute values of the circumsolar radiance cannot be explained without aerosol particles. With regard to the absolute value and the color ratio, these measurements distinctly differ from the circumsolar sky radiation of the Rayleigh atmosphere; the absolute values of the measured radiance are by more than 50 % higher than the absolute values of the circumsolar radiance of the Rayleigh atmosphere which have been computed under consideration of multiple scattering.

The exponent of the aerosol size distribution which results from the analysis of the sky radiation measurements taken in Hawaii, is $\nu^* = 4.0$. In case of subsidence, almost the same exponent is valid for the aerosol size distributions found at Mainz and the Jungraujoch. This is at least true for the size range $r \leqslant 1\ \mu$, if the effect of the strong air pollution is disregarded. According to the theory, the aerosol size distribution resulting from the comparison between the measurements and the theory, represents a mean value of the atmosphere. Generally, the aerosol size distributions which have been measured near the continental earth's surface, have an exponent $\nu^* = 3.0$ (Junge, 1963). The aerosol size distributions which have been measured by Jaenicke (1966) simultaneously with the circumsolar sky radiation on top of the Haleakala, Hawaii, also show an exponent $\nu^* \approx 3.0$. This implies that the model which is based upon a constant exponent ν^* of the aerosol size distribution with height, must be amended, since the exponent ν^* is a function of height.

As mentioned before, the measured exponent ν^* is the mean value for the aerosol size distributions of the entire atmosphere. This mean value is larger than the exponent which has been obtained by direct measurements of the aerosol size distribution at the observation site. This implies that the exponent increases with height. From the theoretical studies, it is very obvious that the exponent depends on the height specially in the size range of the giant particles ($r \geqslant 1\ \mu$) as a consequence of sedimentation (Junge, 1963). However, this height dependence seems also to be valid for the size range $r < 1\ \mu$ as it has been proved by the analysis of the measurements of sky radiation, discussed in this paper.

Acknowledgements

The author has been encouraged by Dr. K. Bullrich to carry out the present investigation.

The European Office of Aerospace Research of the U.S. Air Force Cambridge Research Laboratories has granted the financial support for the construction of the apparatus and the accomplishment of the investigations (Contract No AF61(052)-595). The stay at the research station Jungfraujoch, Switzerland, was sponsored by the Deutsche Forschungsgemeinschaft.

The stay on the island Maui, Hawaii, has been financially supported by the European Research Office of the U.S. Department of the Army (Contract No DA-91-591-EUC-3458). Professors Dr. Jefferies and Dr. Steiger of the Institute of Geophysics of the University of Hawaii made it possible to use the technical facilities of the Haleakala Observatory. The mechanical parts of the apparatus have been manufactured by Mr. K. Dröll in the workshop of the Mainz Institute.

The author wishes to express his thanks to all these persons and organizations for their assistance and cooperation.

REFERENCES

de Bary, E. 1964. Influence of multiple scattering on the intensity and polarization of diffuse sky radiation. *Appl. Optics 3*, 1293–1303.

de Bary, E., Braun, B. & Bullrich, K. 1965. *Tables Related to Light Scattering in a Turbid Atmopshere*, vol. I–III. Air Force Cambridge Research Lab. Special Rept. No. 33.

Bullrich, K., de Bary, E. & Möller, F. 1952. Die Farbe des Himmels. *Geofis. Pura Appl. 23*, 66–110.

Bullrich, K. & Eiden, R. 1964. Optical transmission of the atmosphere in Hawaii. Final technical report. Contract DA-91-EUC-2964.

Bullrich, K., Eiden, R., Jaenicke, R. & Nowak, W. 1966. Optical transmission of the atmosphere in Hawaii. II. Final technical report. Contract DA-91-591-EUC-3458. *Geofis. Pura Appl.* In press.

Bugnolo, D S. 1960. On the question of multiple scattering in the troposphere. *J. of Geophys. Res. 65*, 879–884.

Coulson, K., Dave, J. & Sekera, Z. 1960. *Tables Related to Radiation from a Planetary Atm. with Rayleigh Scattering.* Univ. of Calif. Press, Berkeley, Los Angeles.

Coulson, K. L., Bouricius, G. M. & Gray, E. L. 1965. Optical reflection properties of natural surfaces. *J. of Geophys. Res. 80*, No. 18, 460–4611.

Danzer, K. & Bullrich, K. 1966. Calculations of the influence of aerosolparticles with certain intervals of radii on the scattering coefficient and the sky radiance. *Optik 24*, 577–594.

Deirmendjian, D. 1959. Theory of the solar aureole (part II). *Ann. de Geophys. 15*, No. 2, 218–249.

Dirmhirn, I. 1964. *Das Strahlungsfeld im Lebensraum.* Akademische Verlagsgesellschaft, Frankfurt/Main.

Eiden, R. 1966. The elliptical polarization of light scattered by a volume of atmospheric air. *Appl. Optics 5*, 569–575.

Eiden, R. 1966. Messungen und Berechnungen der spektralen sonnennahen Himmelsstrahlung mit Hilfe neuer experimenteller und theoretischer Methoden. Dissertation. Mainz.

Günther, S. 1949. Die Himmelshelligkeit in der Nähe der Sonne. *Optik 5*, 240–257.

Hänel, G. 1967. Vorbereitende Studien zur Messung des Brechungsindex atmosphärischer Aerosolteilchen mit vorläufigen Messergebnissen des Realteils bei verschiedenen relativen Luftfeuchtigkeiten. Diplomarbeit. Mainz.

van de Hulst, H. C. 1957. *Light Scattering by Small Particles.* John Wiley and Sons, New York.

Jaenicke, R. & Junge, Chr. 1966. Studien zur oberen Grenzgrösse des natürlichen Aerosols. *Beitr. Phys. Atmos.* In press.

Junge, Chr. E. 1952. Gesetzmässigkeiten in der Grössenverteilung atmosphärischer Aerosole über dem Kontinent. Ber. Dtsch. Wetterdienst U.S. Zone, No. 35, pp. 261–276.

Junge, Chr. E. 1963. *Air Chemistry and Radioactivity.* Academic Press, New York and London.

Kasten, F. 1962. Sichtweite und Albedo, insbesondere im Polargebiet. II. *Beitr. Phys. Atm. 35*, 18–42.

Middleton, W. E. K. & Mungall, A. G. 1952. The luminous directional reflectance of snow. *J. of Opt. Soc. 42*, No. 8, 572–579.

Mie, G. 1908. Beiträge zur Optik trüber Medien. *Ann. Phs. 25*, 377–445.

Möller, F., de Bary, E. & Bullrich, K. 1954. Beiträge zur Erklärung von Himmelsfarbe und Helligkeit. *Z. Meteor. 8*, 303.

Newkirk, G. & Eddy, J. A. 1964. Light scattering by particles in the upper atmosphere. *J. of Atm. Sciences 21*, 35–60.

Robinson, E. 1962. Effects of air pollution on visivility. In *Air Pollution*, vol. I. Hersg. A. C. Stern. Academic Press, New York and London.

Sekihara, K. & Murai, M. 1961. On the measurement of atmospheric extinction of solar radiation and the sun's aureole. *Met. and Geophys. 7*, 557–74.

Spänkuch, D. 1965. Über den Einfluss der Dunstschichtung auf die Strahldichteverteilung des wolkenlosen Himmels. *Z. Meteor. 17*, 202–208.

Volz, F. 1954. Die Optik und Meteorologie der atmosphärischen Trübung. Ber. Dtsch. Wetterdienstes, No. 13, vol. 2.

Volz, F. 1956. Optik des Dunstes. In *Handbuch der Geophys.*, Vol. VIII. Berlin.

Volz, F. 1961. Photometer mit Selen-Photoelement zur spektralen Messung der Sonnenstrahlung und zur Bestimmung der Wellenlängenabhängigkeit der Dunsttrübung. *Arch. Met. Geophys. Biokl. 10*, 100.

ВЫЧИСЛЕНИЯ И ИЗМЕРЕНИЯ СПЕКТРАЛЬНОГО ХОДА ЯРКОСТИ В СОЛНЕЧНОМ ОРЕОЛЕ

Обсуждается применение теории однократного рассеяния для описания и интерпретации спектрального хода яркости неба. Показано, что в солнечном ореоле влиянием рассеяний высших порядков можно пренебречь.

Теоретические расчеты спектрального хода яркости неба, проведенные Булльрихом и др. (1965) на основе экспоненциального закона распределения аэрозоля по размерам с верхней границей радиусов частиц $r = 10$ мкм, продолжены до $r = 150$ мкм. Анализ показывает, что аэрозольные частицы с $r > 30$ мкм не влияют на яркость неба.

Путем сравнения с теоретическими результатами были проанализированы и интерпретированы измерения, проведенные в Майнце, Германия, на исследовательской станции Юнгфрау в Верхних Альпах, Швейцария, и на о. Мауи, Гавайские о-ва. Некоторые измерения потребовали модификации модели замутненной атмосферы. Показатель экспоненты в распределении аэрозоля по размерам, рассматриваемый обычно как постоянная, должен зависеть от размера частиц. Далее было найдено, что этот показатель есть функция высоты (возрастает с высотой).